Space-Time Discontinuous Galerkin Finite Element Method for Hyperbolic Conservation Laws

Jaap van der Vegt

University of Twente

Ph.D. Course

Eötvös Lorand University Budapest, March, 2004

Space-Time Discontinuous Galerkin Finite Element Methods

Original motivation of research:

Aerodynamical applications, such as helicopters, manoeuvering aircraft and fluid-structure interaction require:

- Improved capturing of vortical structures and flow discontinuities, such as shocks.
- Moving and deforming flow domains.
- Capability to deal with complex geometries.
- High computational efficiency for unsteady flow simulations.

Helicopter Rotor Wake

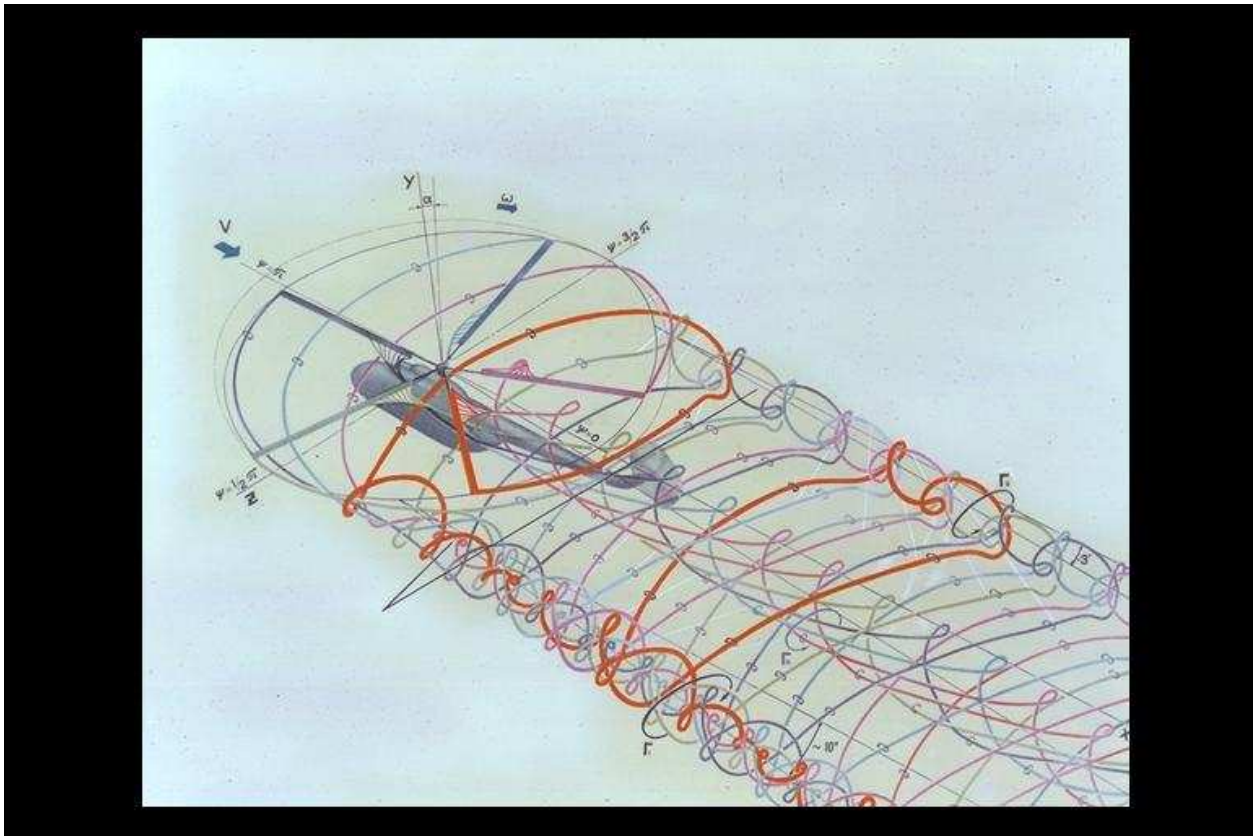

Wake of a helicopter rotor (NASA).

Delta Wing Vortices

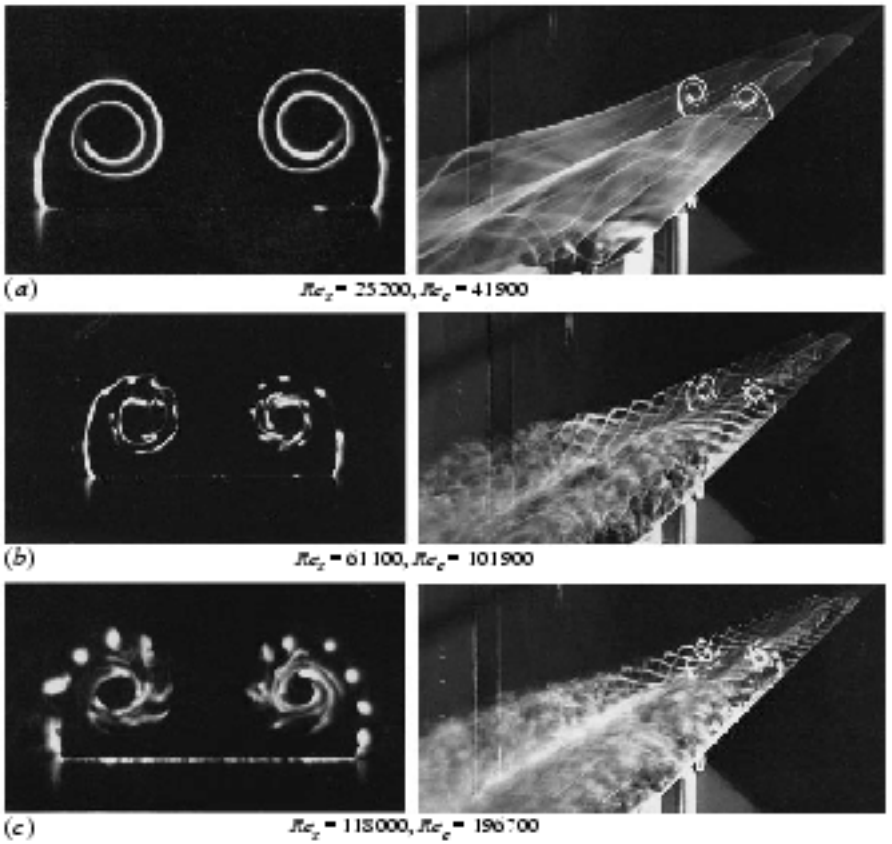

Vortical structures generated by a delta wing (A.J. Riley and M.V. Lowson, *J. of Fluid Mechanics* **369**:49, 1998).

Shock Waves

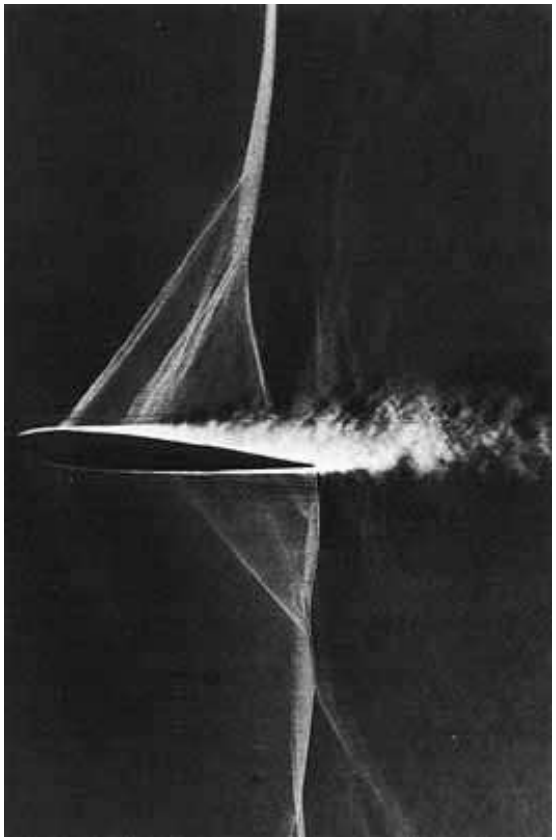

Unsteady transonic flow over an airfoil with boundary layer separation (NASA).

Motivation of Present Research (continued)

More recent research topics:

- Wet chemical etching of microstructures
- Two-phase and chemically reacting flows
- Large-eddy simulation of turbulent flows: variational multiscale analysis
- Water waves
- Maxwell equations

Objectives

To develop a numerical scheme for hyperbolic conservation laws with the following properties:

- Conservative numerical discretization on moving and deforming meshes (satisfy geometric conservation law)
- Improve accuracy with grid adaptation using local grid refinement
- Maintain accuracy on irregular meshes
- Efficient capturing of discontinuities
- Easy to parallelize

These requirements have been the primary motivation to develop discontinuous Galerkin finite element methods.

Objectives

In addition, we want to be able to deal with (but not discussed in these lectures):

- Parabolic and incompletely parabolic PDEs.
- h-p mesh adaptation.
- Free surface problems.
- Develop special elements, for instance with divergence free basis functions.

Overview of Lecture

- One-dimensional example: scalar conservation laws
  - weak formulation
  - numerical flux
  - solution of non-linear coefficient equations
  - stability analysis of pseudo-time integration
- Space-time discontinuous Galerkin finite element discretization for hyperbolic conservation laws with application to the Euler equations of gas dynamics:
  - ALE form of weak formulation
  - numerical flux
  - stabilization operator

Time-Dependent Flow Domain

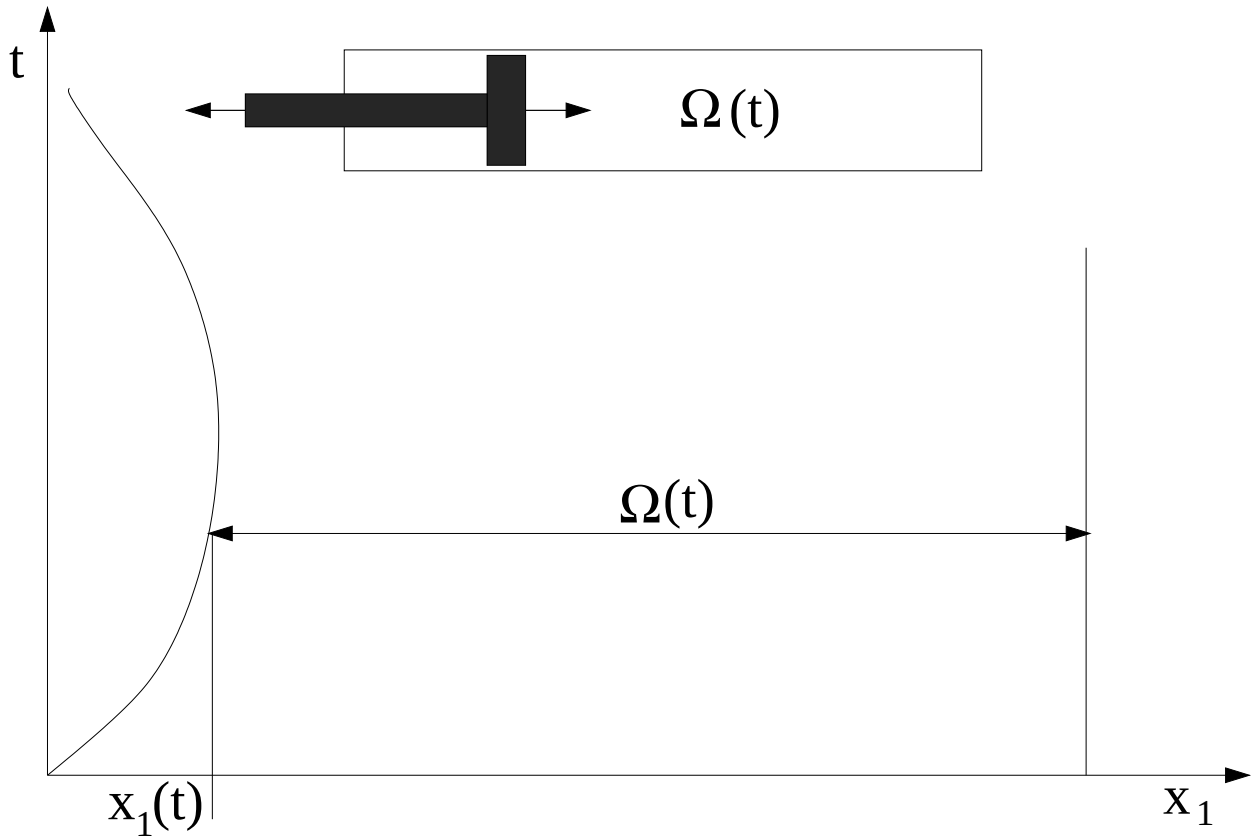

Example of a time dependent flow domain $\Omega(t)$.

Scalar Conservation Laws

- Consider the scalar conservation law in the time dependent flow domain $\Omega \subseteq \mathbb{R}$:

$$\frac{\partial u}{\partial t} + \frac{\partial f(u)}{\partial x_1} = 0, \qquad x_1 \in \Omega(t),\ t \in (t_0, T),$$

with boundary conditions:

$$u(x_1, t) = \mathcal{B}(u, u_w), \qquad x_1 \in \partial\Omega(t),\ t \in (t_0, T),$$

and initial condition:

$$u(x_1, 0) = u_0(x_1), \qquad x_1 \in \Omega(t_0).$$

Space-Time Domain

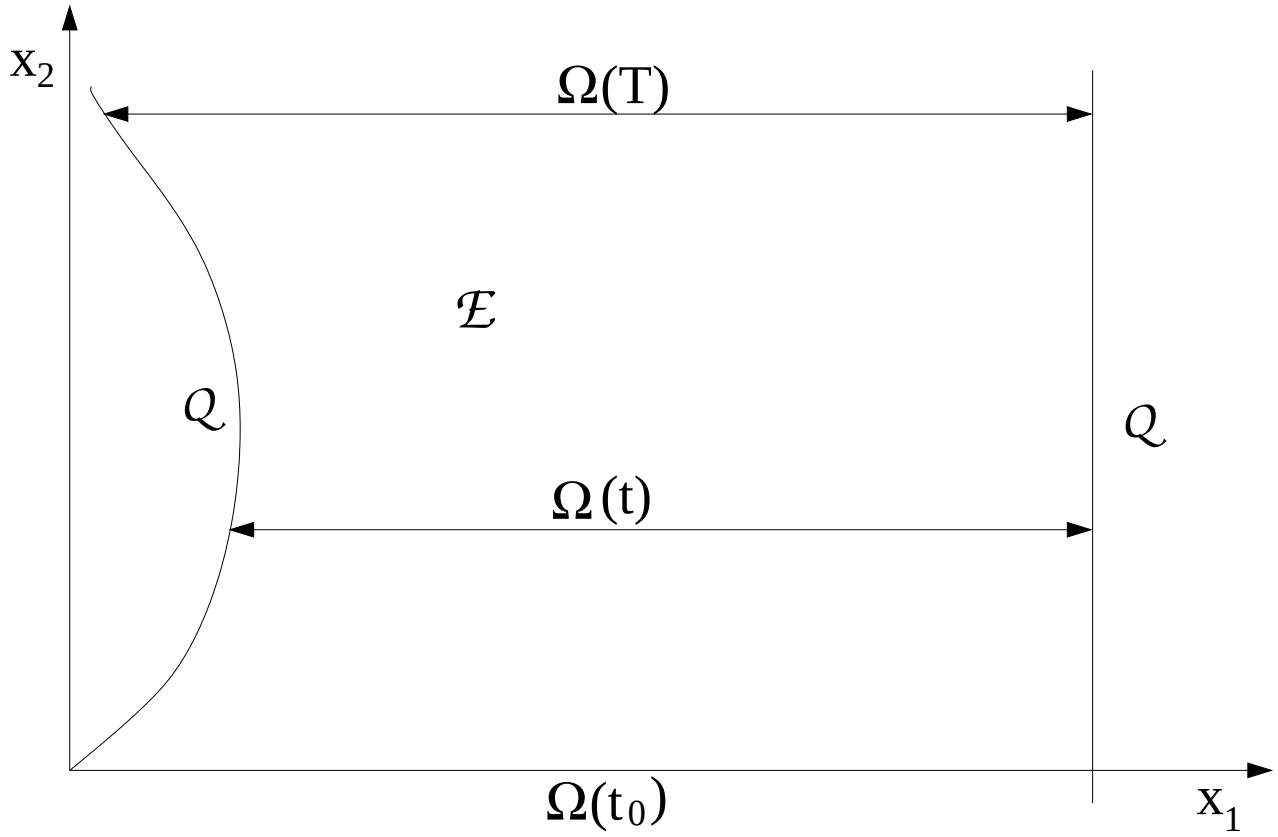

Example of a space-time domain $\mathcal{E}$.

Definition of Space-Time Domain

- Let $\mathcal{E} \subset \mathbb{R}^2$ be an open domain.
- A point $x \in \mathbb{R}^2$ has coordinates (x_1, x_2), where x_1 is the spatial coordinate and x_2 represents time.
- Define the flow domain Ω at time t as:

$$\Omega(t) := \{x_1 \in \mathbb{R} \,|\, (x_1, t) \in \mathcal{E}\}$$

- Define the boundary $\mathcal{Q}$ as:

$$\mathcal{Q} := \{x \in \partial\mathcal{E} \,|\, t_0 < x_2 < T\}$$

- **Note :** The space-time domain boundary $\partial\mathcal{E}$ is equal to:

$$\partial\mathcal{E} = \Omega(t_0) \cup \mathcal{Q} \cup \Omega(T).$$

Space-Time Formulation of Scalar Conservation Law

- Define the space-time flux vector: $\mathcal{F}(u) := (f(u), u)^T$, then the scalar conservation law can be written as:

$$\operatorname{div} \mathcal{F}(u(x)) = 0, \qquad x \in \mathcal{E}$$

with boundary conditions:

$$u(x) = \mathcal{B}(u, u_w), \qquad x \in \mathcal{Q},$$

and initial condition:

$$u(x) = u_0(x), \qquad x \in \Omega(t_0).$$

- The div operator is defined as: $\operatorname{div} \mathcal{F} = \frac{\partial \mathcal{F}_i}{\partial x_i}$.

Space-Time Slab

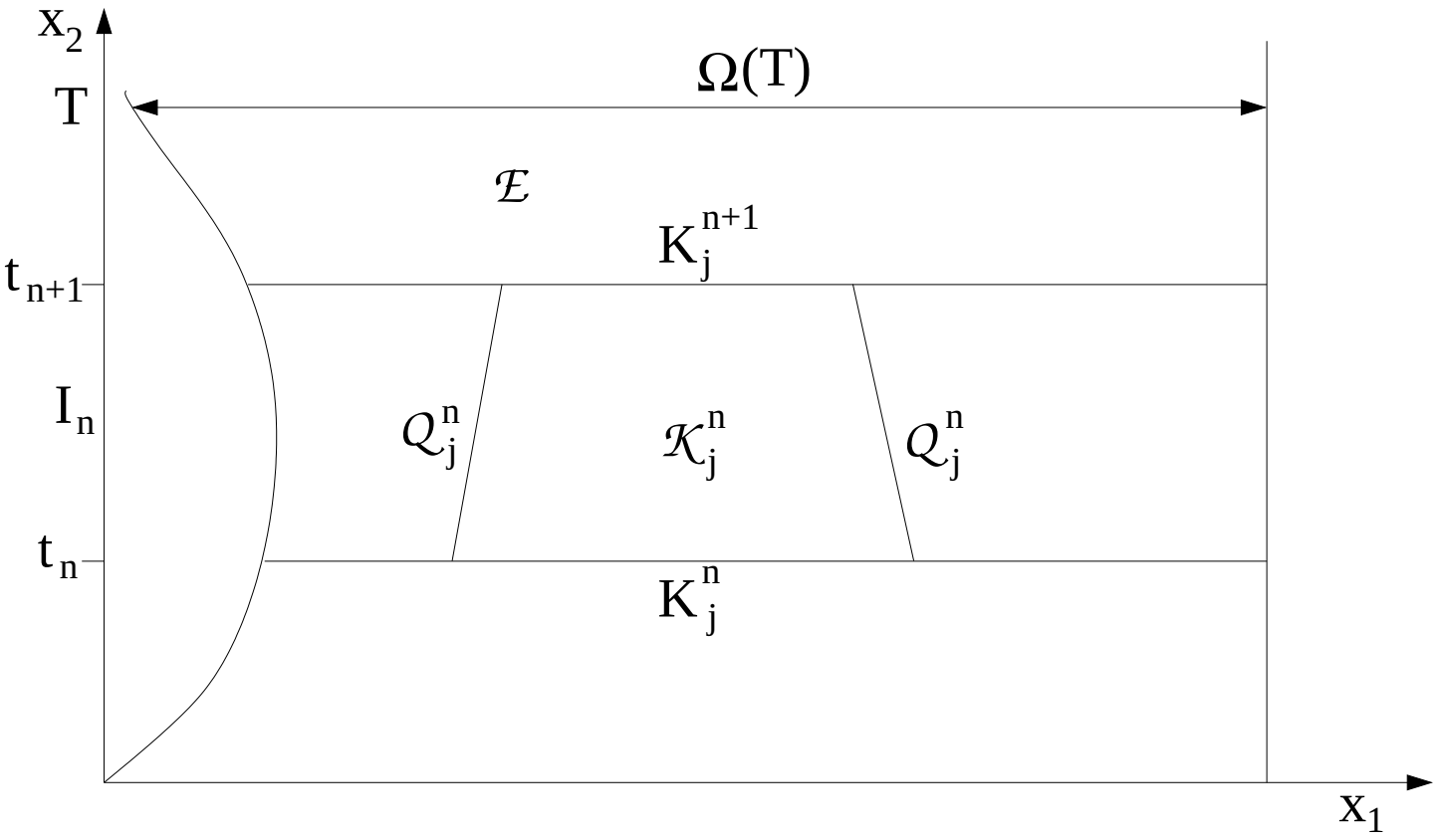

Space-time slab in space-time domain $\mathcal{E}$.

Definition of Space-Time Slab

- Consider a partitioning of the time interval (t_0, T): $\{t_n\}_{n=0}^{N}$, and set $I_n = (t_n, t_{n+1})$.
- Define a space-time slab as: $\mathcal{I}_n := \{x \in \mathcal{E} \mid x_2 \in I_n\}$
- Split the space-time slab into non-overlapping elements: $\mathcal{K}_j^n$.
- We will also use the notation: $K_j^n = \mathcal{K}_j^n \cap \{t_n\}$ and $K_j^{n+1} = \mathcal{K}_j^n \cap \{t_{n+1}\}$

Geometry of Space-Time Element

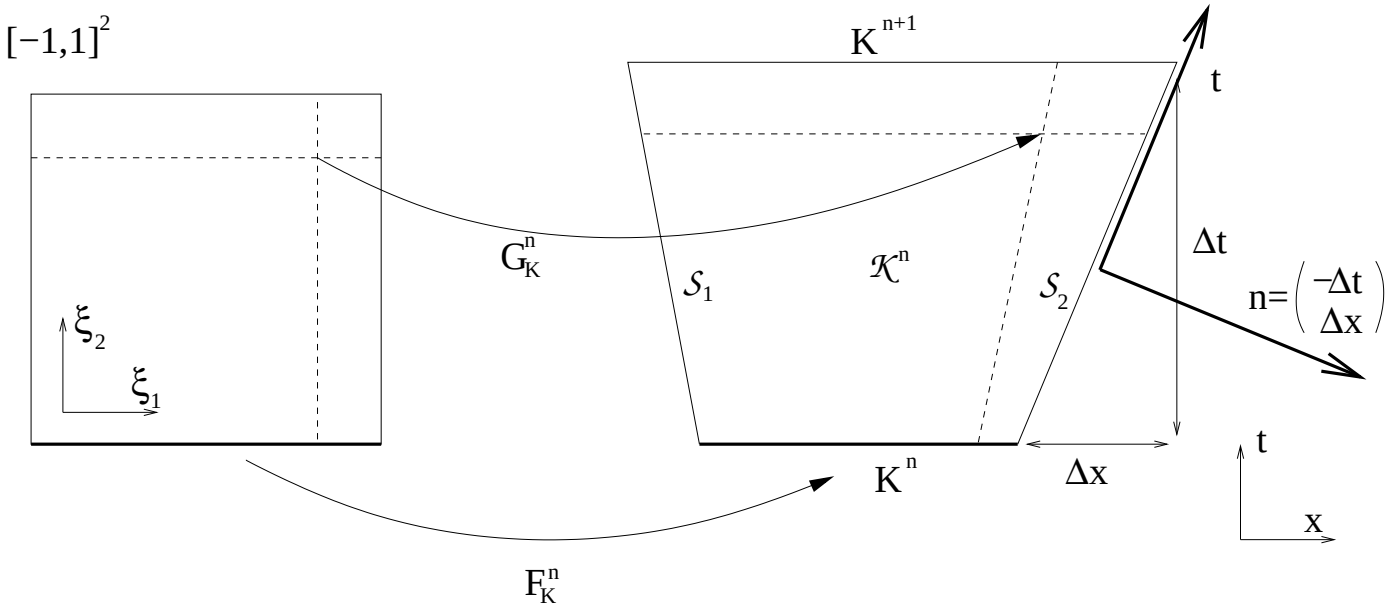

Geometry of 2D space-time element in both computational and physical space.

Space-Time Element Definition

Definition of the mapping G_K^n which the connects the space-time element $\mathcal{K}^n$ to the reference element $\hat{\mathcal{K}} = [-1, 1]^2$:

- Define a smooth, orientation preserving and invertible mapping Φ_t^n in the interval I_n as:
$$\Phi_t^n : \Omega(t_n) \rightarrow \Omega(t) : x_1 \mapsto \Phi_t^n(x_1), \quad t \in I_n.$$
- Split $\Omega(t_n)$ into the tessellation $\bar{\mathcal{T}}_h^n$ with non-overlapping elements K_j.
- Define $\chi_i(\xi_1), \xi_1 \in [-1, 1]$ as the standard linear finite element shape functions:

$$\chi_1(\xi_1) = \tfrac{1}{2}(1 - \xi_1),$$
$$\chi_2(\xi_1) = \tfrac{1}{2}(1 + \xi_1).$$

Space-Time Element Definition (continued)

- The mapping F_K^n is defined as:

$$F_K^n : [-1,1] \rightarrow K^n : \xi_1 \longmapsto \sum_{i=1}^{2} x_i(K^n)\chi_i(\xi_1),$$

with $x_i(K^n)$ the spatial coordinates of the space-time element at time $t = t_n$.

- Similarly we define the mapping F_K^{n+1}:

$$F_K^{n+1} : [-1,1] \rightarrow K^{n+1} : \xi_1 \longmapsto \sum_{i=1}^{2} \Phi_{t_{n+1}}^{n}(x_i(K^n))\chi_i(\xi_1).$$

Space-Time Element Definition (continued)

- The space-time element is defined by linear interpolation in time:

$$G_K^n : [-1,1]^2 \rightarrow \mathcal{K}^n : (\xi_1, \xi_2) \longmapsto (x_1, x_2),$$

with:

$$(x_1, x_2) = \Big(\tfrac{1}{2}(1-\xi_2) F_K^n(\xi_1) + \tfrac{1}{2}(1+\xi_2) F_K^{n+1}(\xi_1),$$
$$\tfrac{1}{2}(t_n + t_{n+1}) + \tfrac{1}{2}(t_n - t_{n+1})\xi_2 \Big).$$

- The space-time tessellation is now defined as:

$$\mathcal{T}_h^n := \{\mathcal{K} = G_k^n(\hat{\mathcal{K}}) \mid K \in \bar{\mathcal{T}}_h^n\}.$$

Discontinous Galerkin Approximation

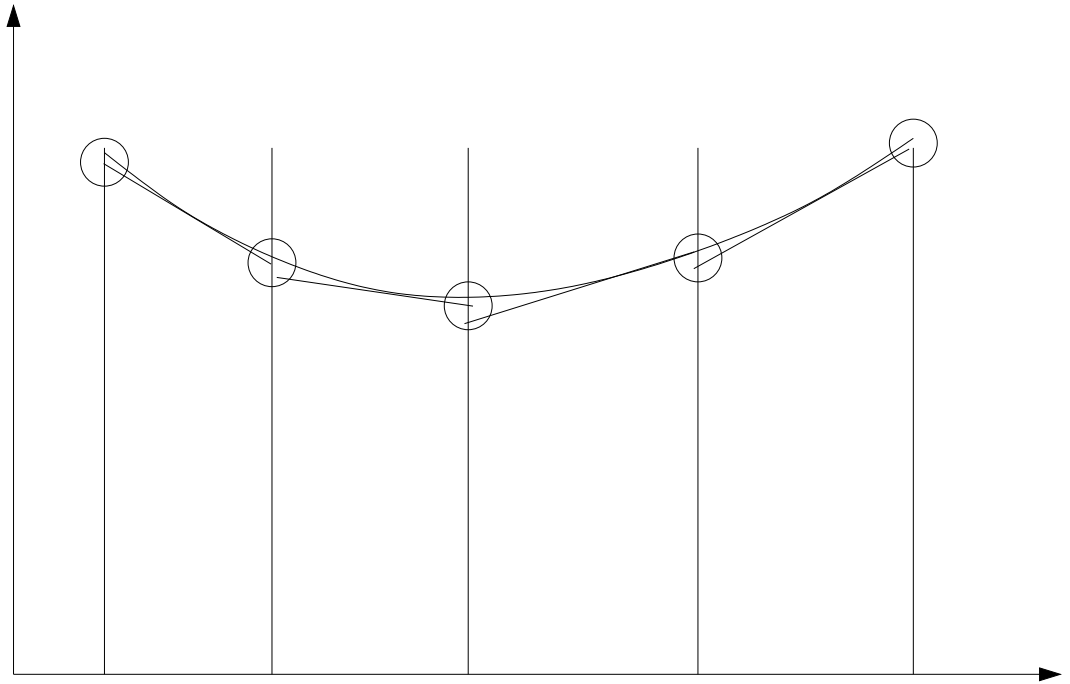

Discontinous Galerkin approximation of a function

Note: The polynomial expansions are discontinuous at element faces.

Basis Functions

- Define in the master element $\hat{\mathcal{K}}$ the basis functions $\hat{\phi}_m, (m = 0, 1, 2)$ as:

$$\begin{aligned} \hat{\phi}_m(\xi_1, \xi_2) &= 1, & m &= 0, \\ &= \xi_m, & m &= 1, 2 \end{aligned}$$

- Define the basis functions ϕ_m in an element $\mathcal{K}$ as:

$$\phi_m(x) = \hat{\phi}_m \circ G_K^{-1}(x).$$

.

Basis Functions (continued)

- Introduce the basis functions $\psi_m : \mathcal{K} \longrightarrow \mathbb{R}$ and split the test and trial functions into an element mean at time t_{n+1} and a fluctuating part:

$$\begin{aligned} \psi(x_1, x_2) &= 1, && m = 0, \\ &= \phi_m(x_1, x_2) - \frac{1}{|K_j(t_{n+1})|} \int_{K_j(t_{n+1})} dK, && m = 1, 2. \end{aligned}$$

- The splitting is beneficial for the definition of the stabilization operator and multigrid convergence acceleration.

Finite Element Space

- Define the finite element space $V_h^1(\mathcal{T}_h^n)$ as:

$$V_h^1(\mathcal{T}_h^n) := \left\{ v_h \,\middle|\, v_h|_{\mathcal{K}_j^n} \in P^1(\mathcal{K}_j^n),\ j = 1, \cdots, N_n \right\},$$

  with $P^1(\mathcal{K}) = \text{span}\{\phi_m, m = 0, 1, 2\}$.

- The trial functions $u_h : \mathcal{T}_h^n \longrightarrow \mathbb{R}^2$ are defined in each element $\mathcal{K} \in \mathcal{T}_h^n$ as:

$$u_h(x) = \mathcal{P}(u(x)|_{\mathcal{K}}) = \sum_{m=0}^{2} \hat{u}_m(\mathcal{K}_j)\psi_m(x), \quad x \in \mathcal{K}_j,$$

  with $\mathcal{P}$ the projection operator to the finite element space $V_h^1(\mathcal{T}_h^n)$ and $\hat{u}_m$ the expansion coefficients.

Finite Element Space (continued)

- **Note :** Since $\int_{K(t_{n+1})} \psi(x) dK = 0$ we have the relation:

$$\bar{u}_h(K_j(t_{n+1}) := \frac{1}{|K(t_{n+1})|} \int_{K(t_{n+1})} dK = \hat{u}_0,$$

and we can write:

$$u_h(x) = \bar{u}_h(K_j(t_{n+1})) + \tilde{u}_h(x),$$

with $\int_{K(t_{n+1})} \tilde{u}(x) dK = 0.$

- One of the main benefits of this splitting is that the equation for $\hat{u}_0$ is very similar to a first order finite volume discretization and is only weakly coupled to the equations for $\tilde{u}_h$.

Weak Formulation for STDG Method

The scalar conservation law can be transformed into a weak formulation:

- Find a $u_h \in V_h^1$, such that for all $w_h \in V_h^1$, we have:

$$\sum_{n=0}^{N_T} \sum_{j=1}^{N_n} \left(\int_{\mathcal{K}_j^n} w_h \, \mathrm{div} \mathcal{F}(u_h) d\mathcal{K} + \int_{\mathcal{K}_j^n} (\mathrm{grad}\, w_h)^T \, \mathfrak{D}(u_h) \, \mathrm{grad}\, u_h d\mathcal{K} \right) = 0.$$

- The second integral with $\mathfrak{D}(u_h) \in \mathbb{R}^2$ is the stabilization operator necessary to obtain monotone solutions near discontinuities.

Weak Formulation (continued)

After integration by parts we obtain the following weak formulation:

- Find a $u_h \in V_h^1$, such that for all $w_h \in V_h^1$, we have:

$$\sum_{n=0}^{N_T} \sum_{j=1}^{N_n} \Big(- \int_{\mathcal{K}_j^n} \operatorname{grad} w_h \cdot \mathcal{F}(u_h) d\mathcal{K} + \int_{\partial \mathcal{K}_j^n} w_h^- n^- \cdot \mathcal{F}(u_h^-) d(\partial \mathcal{K}) + \int_{\mathcal{K}_j^n} (\operatorname{grad} w_h)^T \mathfrak{D}(u_h) \operatorname{grad} u_h d\mathcal{K} \Big) = 0.$$

Traces

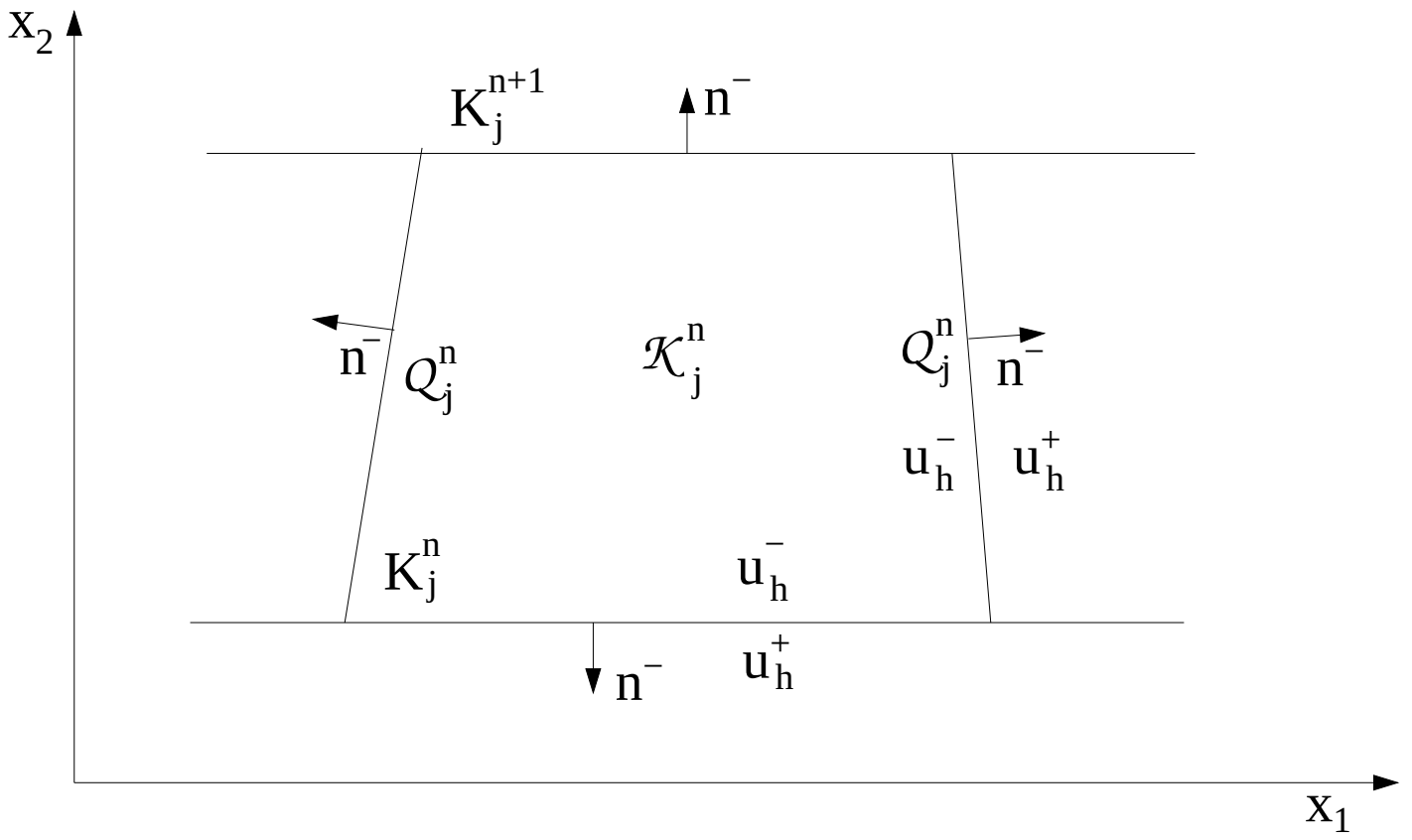

Definition of the traces in a space-time slab.

Numerical Fluxes

- The integrals over the faces $\partial\mathcal{K}$ in the weak formulation are counted twice into summation over the elements, since two elements are connected to each face when we extend the mesh with ghostcells to account for the domain boundary faces.
- We can transform the boundary integrals into:

$$\sum_{\mathcal{K}} \int_{\partial\mathcal{K}} w_h^- \mathcal{F}^- d(\partial\mathcal{K}) = \sum_{\mathcal{S}} \int_{\mathcal{S}} \tfrac{1}{2}(w_h^- n^- + w_h^+ n^+)(\mathcal{F}^- + \mathcal{F}^+) + \tfrac{1}{2}(w_h^- + w_h^+)(\mathcal{F}^- n^- + \mathcal{F}^+ n^+) d\mathcal{S}, \quad (1)$$

with $\mathcal{F}^\pm = \mathcal{F}(u_h^\pm)$, and n^-, n^+ the normal vectors at each side of the face $\mathcal{S}$, which satisfy $n^+ = -n^-$.

Numerical Fluxes

- The formulation must be conservative, which imposes the condition:

$$\int_{\mathcal{S}} w_h n^- \mathcal{F}^- d\mathcal{S} = -\int_{\mathcal{S}} w_h n^+ \mathcal{F}^+ d\mathcal{S}, \qquad \forall w_h \in V_h^1(\mathcal{T}_h^n),$$

  hence the second contribution in (1) is zero.

- The boundary integrals therefore are equal to:

$$\sum_{\mathcal{K}} \int_{\partial\mathcal{K}} w_h^- \mathcal{F}^- d(\partial\mathcal{K}) = \sum_{\mathcal{S}} \int_{\mathcal{S}} \tfrac{1}{2}(w_h^- - w_h^+) n^- (\mathcal{F}^- + \mathcal{F}^+) d\mathcal{S},$$

  using the relation $n^+ = -n^-$.

Numerical Fluxes

- Replace the multi-valued trace of the flux at $\mathcal{S}$ with a numerical flux function:

$$H(u_h^-, u_h^+, n) = \tfrac{1}{2} n \cdot (\mathcal{F}^- + \mathcal{F}^+),$$

then we obtain the relation:

$$\begin{aligned}\sum_{\mathcal{K}} \int_{\partial\mathcal{K}} w_h^- \mathcal{F}^- d(\partial\mathcal{K}) &= \sum_{\mathcal{S}} \int_{\mathcal{S}} (w_h^- - w_h^+) H(u_h^-, u_h^+, n^-) d\mathcal{S} \\ &= \sum_{\mathcal{K}} \int_{\partial\mathcal{K}} w_h^- H(u_h^-, u_h^+, n^-) d(\partial\mathcal{K}),\end{aligned}$$

using the relation $H(u_h^-, u_h^+, n^-) = -H(u_h^+, u_h^-, n^+)$.

Numerical Fluxes

- The numerical flux at the boundary faces $K_j(t_n)$ and $K_j(t_{n+1})$, which have as normal vectors $n^- = (0, \mp 1)^T$, respectively, is defined as:

$$\begin{aligned} H(u_h^-, u_h^+, n^-) &= u_h^+ \qquad \text{at } K_j(t_n) \\ &= u_h^- \qquad \text{at } K_j(t_{n+1}). \end{aligned}$$

- The numerical flux at the boundary faces $\mathcal{Q}_j^n$ is a monotone Lipschitz $H(u_h^-, u_h^+, n)$ which is consistent:

$$H(u, u, n) = n \cdot \mathcal{F}(u)$$

and conservative:

$$H(u_h^-, u_h^+, n^-) = -H(u_h^+, u_h^-, n^+).$$

Riemann Problem

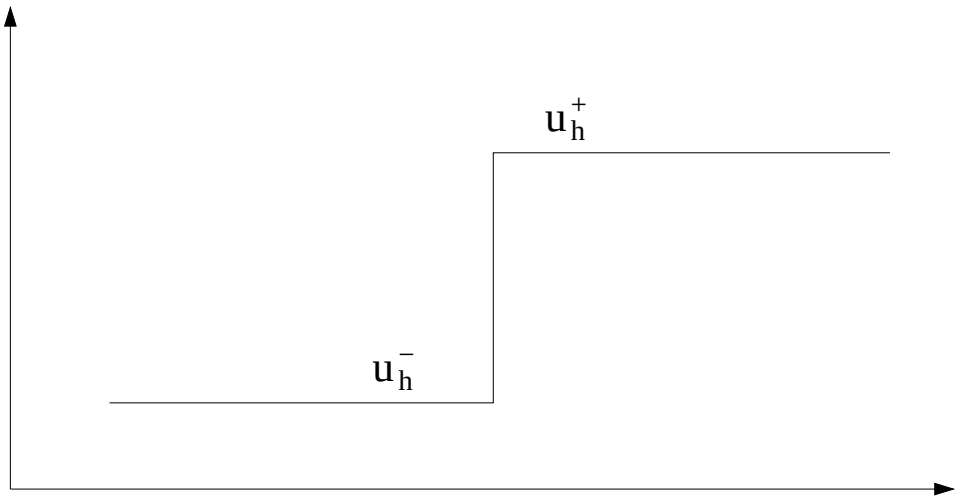

Initial state in Riemann problem

- The monotone Lipschitz flux $H(u_h^-, u_h^+, n)$ is obtained by (approximately) solving the Riemann problem with initial states u_h^- and u_h^+ at the element faces $\mathcal{Q}_j^n$.
- This procedure introduces upwinding into the discontinuous Galerkin finite element method.

Upwind Fluxes

Consistent, monotone Lipschitz fluxes are:

- Godunov flux
- Engquist-Osher flux
- Lax-Friedrichs flux
- Roe flux with 'entropy fix'
- **HLLC flux**

The choice which numerical flux should be used depends on many aspects, e.g. accuracy, robustness, computational complexity, and personal preference.

Weak Formulation DG Discretization

After introducing the numerical fluxes we can transform the weak formulation into:

- Find a $u_h \in V_h^1(\mathcal{T}_h^n)$, such that for all $w_h \in V_h^1(\mathcal{T}_h^n)$, the following variational equation is satisfied:

$$\sum_{j=1}^{N_n} \Big(- \int_{\mathcal{K}_j^n} (\operatorname{grad} w_h) \cdot \mathcal{F}(u_h) d\mathcal{K} + \int_{K_j(t_{n+1})} w_h^- u_h^- dK - \int_{K_j(t_n)} w_h^- u_h^+ dK + \int_{\mathcal{Q}_j^n} w_h^- H(u_h^-, u_h^+, n^-) d\mathcal{Q} + \int_{\mathcal{K}_j^n} (\operatorname{grad} w_h)^T \mathfrak{D}(u_h) \operatorname{grad} u_h \, d\mathcal{K} \Big) = 0.$$

- **Note:** Due to the causality of the time-flux the solution in a space-time slab only depends explicitly on the data from the previous space-time slab.

DG-Expansion Coefficient Equations for Element Mean

- Introduce the polynomial expansions for u_h and w_h into the weak formulation and the fact that the coefficients $\hat{w}_m$ are arbitrary, then the following set of equations for the element mean $\bar{u}_h(K_j(t_{n+1}))$ is obtained:

$$\big|K_j(t_{n+1})\big|\bar{u}_h(K_j(t_{n+1}))-\big|K_j(t_n)\big|\bar{u}_h(K_j(t_n))+\int_{\mathcal{Q}_j^n} H(u_h^-,u_h^+,n^-)d\mathcal{Q}=0.$$

- These equations are equivalent to a first order accurate finite volume formulation, except that more accurate data are used at the element faces.

DG-Expansion Coefficient Equations for Element Fluctuations

- The equations for the coefficients $\hat{u}_m(\mathcal{K}_j^n)$, $(m = 1, 2)$ for the fluctuating part of the flow field $\tilde{u}_h$ are equal to:

$$\sum_{m=1}^{2} \hat{u}_m(\mathcal{K}_j^n)\Big(- \int_{\mathcal{K}_j^n} \frac{\partial \psi_l}{\partial t}\psi_m d\mathcal{K} + \int_{K_j^{n+1}} \psi_l(x_1, t_{n+1}^-)\psi_m(x_1, t_{n+1}^-) dK$$

$$+ \int_{\mathcal{K}_j^n} \frac{\partial \psi_l}{\partial x_k}\mathfrak{D}_{kp}(u_h)\frac{\partial \psi_m}{\partial x_p} d\mathcal{K}\Big)$$

$$- \int_{K_j^n} u_h(x_1, t_n^-)\psi_l(x_1, t_n^+) dK - \bar{u}_h(K_j^{n+1}) \int_{\mathcal{K}_j^n} \frac{\partial \psi_l}{\partial t} d\mathcal{K}$$

$$+ \int_{\mathcal{Q}_j^n} \psi_l H(u_h^-, u_h^+, n^-) d\mathcal{Q} - \int_{\mathcal{K}_j^n} \frac{\partial \psi_l}{\partial x_1}\mathcal{F}_1(u_h) d\mathcal{K} = 0, \qquad l = 1, 2.$$

Solution of DG Expansion Coefficient Equations

- The space-time DG formulation results in an implicit time-integration scheme.
- The equations for the DG expansion coefficients are represented as:

$$\mathcal{L}(\hat{u}^n, \hat{u}^{n-1}) = 0.$$

- The non-linear equations for the expansion coefficients $\hat{u}^n$ are solved by introducing a pseudo-time τ and marching the solution with a Runge-Kutta method to a steady state:

$$\frac{\partial \hat{u}^*(\mathcal{K}_j^n)}{\partial \tau} = \frac{1}{\triangle t}\mathcal{L}(\hat{u}^*, \hat{u}^{n-1}).$$

- Convergence to steady state in pseudo-time is accelerated using a FAS multigrid procedure.

Runge-Kutta Scheme for Pseudo-Time Integration

For the pseudo-time integration we use a point-implicit five stage Runge-Kutta scheme:

- Initialize the first Runge-Kutta stage: $\hat{v}^{(0)} = \hat{w}^k$.
- Do for all stages $s = 1$ to 5:

$$(1 + \alpha_s \bar{\lambda})\hat{v}^{(s)} = \hat{V}^{(0)} + \alpha_s \bar{\lambda}\Big(\hat{v}^{(s-1)} - \mathcal{L}^k(\hat{v}^{(s-1)}, \hat{u}^k(\mathcal{K}^{n-1}))\Big)$$

- End do
- Update solution: $\hat{w}^k = \hat{v}^{(5)}$.

with $\bar{\lambda} = \triangle\tau/\triangle t$. The Runge-Kutta coefficients are:

$\alpha_1 = 0.0791451$, $\alpha_2 = 0.163551$, $\alpha_3 = 0.283663$, $\alpha_4 = 0.5$, and $\alpha_5 = 1.0$.

Stability Analysis of Pseudo-Time Integration for Linear Advection Equation

- Consider the linear advection equation:

$$u_t + a u_x = 0,$$

  with $a > 0$.

- If we assume a uniform mesh size then the space-time discontinuous Galerkin discretization is equal to:

$$\mathcal{L}(\hat{u}(\mathcal{K}^n), \hat{u}(\mathcal{K}^{n-1})) = \mathcal{A}\hat{u}(\mathcal{K}_j^n) - \mathcal{B}\hat{u}(\mathcal{K}_{j-1}^n) - \mathcal{C}\hat{u}(\mathcal{K}_j^{n-1}).$$

Stability Analysis of Pseudo-Time Integration for Linear Advection Equation

- The matrices $\mathcal{A}$, $\mathcal{B}$, $\mathcal{C}$ in the space-time discontinuous Galerkin discretization are defined as:

$$\mathcal{A} = \begin{pmatrix} 1+\delta & \delta & -\delta \\ -\delta & \frac{1}{3}+\delta & \delta \\ -2-\delta & -\delta & 2+\frac{4}{3}\delta \end{pmatrix}, \quad \mathcal{B} = \begin{pmatrix} \delta & \delta & -\delta \\ -\delta & -\delta & \delta \\ -\delta & -\delta & \frac{4}{3}\delta \end{pmatrix},$$

$$\mathcal{C} = \begin{pmatrix} 1 & 0 & 0 \\ 0 & \frac{1}{3} & 0 \\ -2 & 0 & 0 \end{pmatrix},$$

with $\delta = a\triangle t/\triangle x$.

Fourier Analysis for Linear Advection Equation

- Consider the spatial Fourier mode: $\hat{U}(\mathcal{K}_j^n) = e^{i\theta j}\hat{U}^F$, the stability of the pseudo-time integration algorithm then is determined by the equation:

$$\frac{d\hat{U}^F}{d\tau} = -\frac{1}{\Delta t}\mathcal{P}(\theta)\hat{U}^F$$

  with $\mathcal{P}(\theta) = \mathcal{A} - e^{-i\theta}\mathcal{B}$.

- The matrix $\mathcal{P}$ can be written as: $\mathcal{P} = QMQ^{-1}$, with Q the matrix of the right eigenvectors and M the diagonal matrix with the eigenvalues $\mu_m(\theta)$ of $\mathcal{P}(\theta)$.

- Introducing a new vector $\hat{V}^F = Q^{-1}\hat{U}^F$, we obtain a system of independent ODEs:

$$\frac{d\hat{V}_m^F}{d\tau} = -\frac{\mu_m(\theta)}{\triangle t}\hat{V}_m^F, \qquad \text{for } m = 0, 1, 2.$$

Fourier Analysis for Linear Advection Equation

- This system of ordinary differential equations is solved with a semi-implicit Runge-Kutta scheme with an amplification factor $G(z)$, which is defined recursively as:

$$G(z) = 1$$

For $s = 1$ to 5

$$G(z) = \frac{1.0 + \alpha_s(\bar{\lambda} + z)G(z)}{1.0 + \alpha_s\bar{\lambda}}$$

End for

- The pseudo-time integration method is stable if:

$$|G(z_m(\theta))| \leq 1$$

with $z_m(\theta) = -\frac{\Delta\tau}{\Delta t}\mu_m(\theta)$.

Stability Analysis of Pseudo-Time Integration for Linear Advection Equation

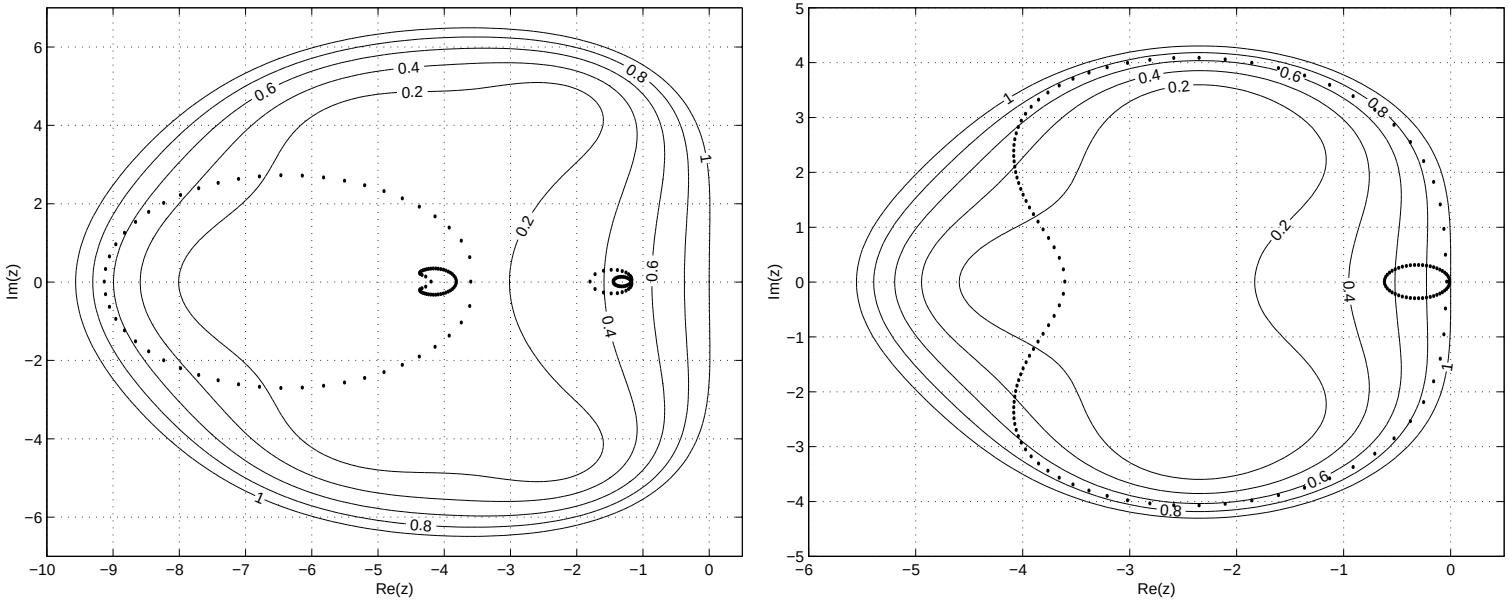

Locus of eigenvalues z_m (dots) of DG discretization of $u_t + au_x = 0$ and stability domain of 5-stage semi-implicit Runge-Kutta method with optimized coefficients. $CFL_{\triangle t} = 1.0$, $CFL_{\triangle \tau} = 1.8$ (left), $CFL_{\triangle t} = 100.0$, $CFL_{\triangle \tau} = 1.8$ (right).

Stability Analysis of Pseudo-Time Integration for Linear Advection Equation

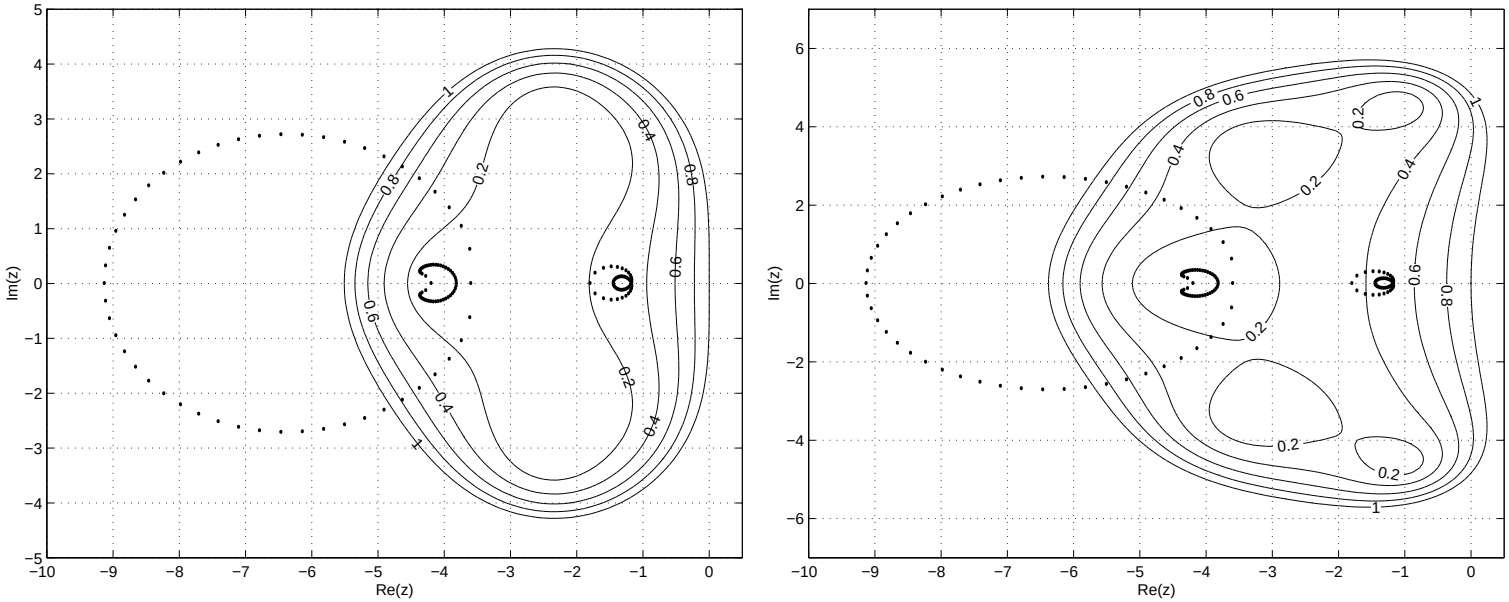

Locus of eigenvalues z_m (dots) of DG discretization of $u_t + au_x = 0$ and stability domain of 5-stage explicit Runge-Kutta method with optimized coefficients (left) and 5-stage semi-implicit Jameson Runge-Kutta scheme (right). $CFL_{\triangle t} = 1.0$. $CFL_{\triangle \tau} = 1.8$.

Properties of DG Methods

The main benefits of discontinuous Galerkin finite elements methods can be summarized as:

- The space-time discontinuous Galerkin finite element method results in a very local, element wise discretization, which has as benefits:
  - the space-time discretization automatically satisfies the geometric conservation law for deforming elements
  - efficient grid adaptation using local grid refinement, no complications caused by hanging nodes and gradient reconstruction
  - combines very well with unstructured grids
  - boundary conditions can be easily implemented using ghost cells

Properties of DG Methods (Continued)

- no special numerical treatment is required to achieve higher order accuracy
- maintains accuracy on irregular grids
- mass matrix for each element is uncoupled from other elements
- efficient parallelization

Geometry of Space-Time Domain for Three-Dimensional Time-Dependent Problems

- Consider an open domain: $\mathcal{E} \subset \mathbb{R}^4$.
- The flow domain $\Omega(t)$ at time t is defined as:

$$\Omega(t) := \{x \in \mathcal{E} \mid x_4 = t,\ t_0 < t < T\}$$

- The space-time domain boundary $\partial\mathcal{E}$ consists of the hypersurfaces:

$$\begin{aligned}\Omega(t_0) :=& \{x \in \partial\mathcal{E} \mid x_4 = t_0\},\\ \Omega(T) :=& \{x \in \partial\mathcal{E} \mid x_4 = T\},\\ \mathcal{Q} :=& \{x \in \partial\mathcal{E} \mid t_0 < x_4 < T\}.\end{aligned}$$

Traces and Computational Mesh

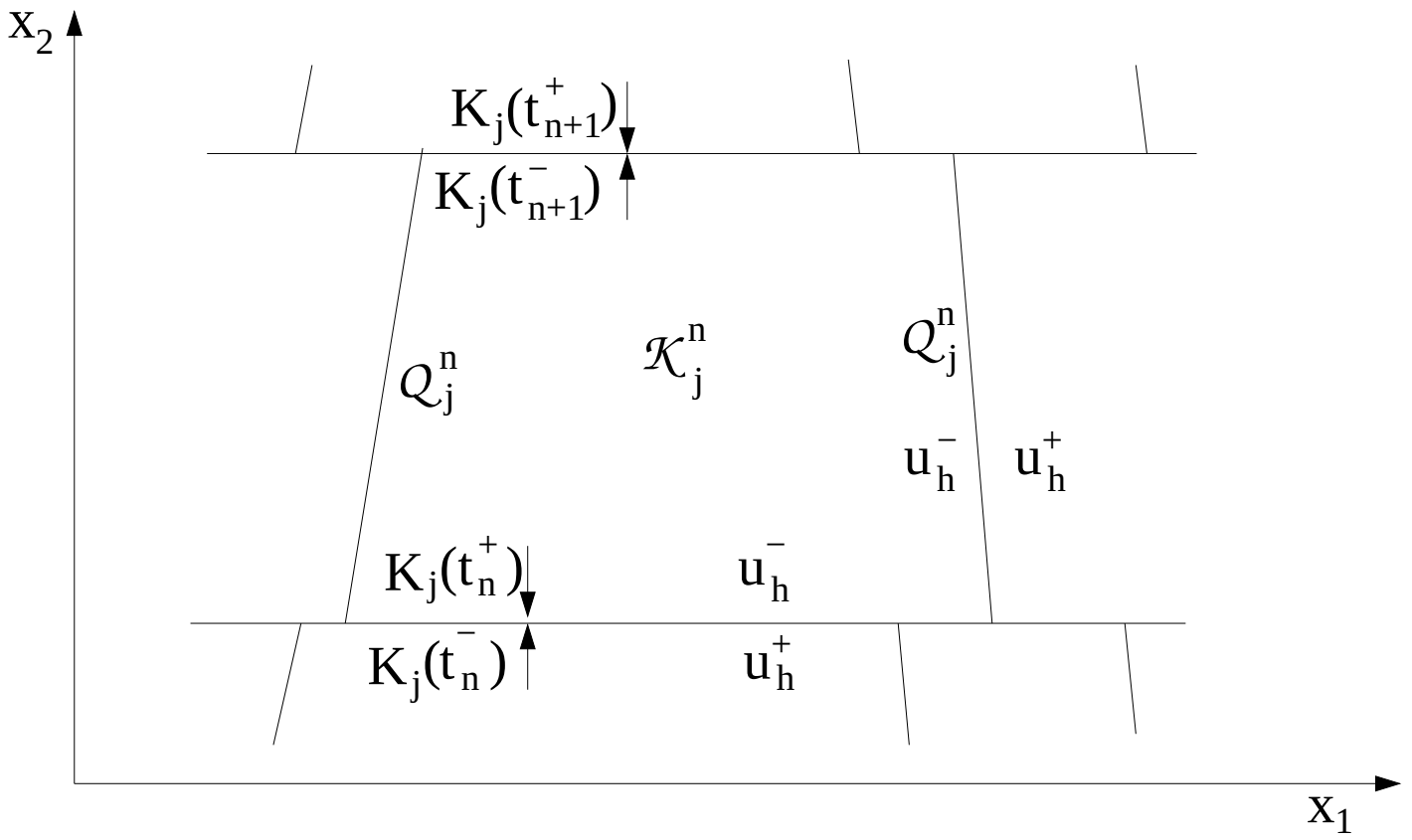

Definition of the traces and computational mesh in an adapted space-time slab.

Hyperbolic Conservation Laws

- Conservation law in space-time domain:

$$\mathrm{div}\mathcal{F}\big(U(x)\big) = 0, \qquad x \in \mathcal{E},$$

  together with the initial and boundary conditions:

$$\begin{aligned} U(x) &= U_0(x), && x \in \Omega(t_0), \\ U(x) &= \mathcal{B}(U, U_w), && x \in \mathcal{Q}. \end{aligned}$$

- Here $U_0 : \Omega(t_0) \longrightarrow \mathbb{R}^n$ denotes the initial flow field, $\mathcal{B} : \mathbb{R}^n \times \mathbb{R}^n \longrightarrow \mathbb{R}^n$ the boundary operator and $U_w : \mathcal{Q} \longrightarrow \mathbb{R}^n$ the prescribed boundary flow field data.

- The divergence of a second order tensor is defined as: $\mathrm{div}\ \mathcal{F} = \frac{\partial \mathcal{F}_{ij}}{\partial x_j}$, and the summation convention is used on repeated indices.

Euler Equations of Gas Dynamics

- The Euler equations of gas dynamics are obtained with:

  $\mathcal{F} : \mathbb{R}^5 \longrightarrow \mathbb{R}^{5\times 4}$ the flux tensor :

$$\mathcal{F} = \begin{pmatrix} \rho u_1 & \rho u_2 & \rho u_3 & \rho \\ \rho u_1^2 + p & \rho u_1 u_2 & \rho u_1 u_3 & \rho u_1 \\ \rho u_1 u_2 & \rho u_2^2 + p & \rho u_2 u_3 & \rho u_2 \\ \rho u_1 u_3 & \rho u_2 u_3 & \rho u_3^2 + p & \rho u_3 \\ (\rho E + p) u_1 & (\rho E + p) u_2 & (\rho E + p) u_3 & \rho E \end{pmatrix}$$

  $U : \mathcal{E} \longrightarrow \mathbb{R}^5$ the vector of conservative flow variables with components:

$$U_i = \mathcal{F}_{i4}$$

- The Euler equations are completed with the ideal gas law:

$$p = (\gamma - 1)\rho(E - \tfrac{1}{2} u \cdot u).$$

Approximation Spaces

- The discontinuous Galerkin finite element discretization is obtained using the finite element space:

$$V_h^1(\mathcal{T}_h^n) := \left\{ U_h \in V(\mathcal{T}_h^n) \;\middle|\; U_h|_{\mathcal{K}} \in (P^1(\mathcal{K}))^5 \right\},$$

  with the polynomial space $P^1(\mathcal{K}) = \text{span}\{\psi_m, m = 0, \cdots, 4\}$.

- The basis functions ψ_m are linear in the reference element $\hat{\mathcal{K}}$ and discontinuous across element faces, both in space and time.

- The trial functions $U_h : \mathcal{T}_h^n \rightarrow \mathbb{R}^5$ are defined in each element $\mathcal{K} \in \mathcal{T}_h^n$ as:

$$U_h(\bar{x}, t)|_{\mathcal{K}} = \sum_{m=0}^{4} \hat{U}_m(\mathcal{K}) \psi_m(\bar{x}, t),$$

  with $\hat{U}_m \in \mathbb{R}^5$ the expansion coefficients.

Basis Functions

- The basis functions ψ_m are constructed such that the test and trial functions in each space-time slab can be split into an element mean $\bar{U}_h : \mathcal{T}_h^n \rightarrow \mathbb{R}^5$ at the time level t_{n+1} and a fluctuating part $\tilde{U}_h : \mathcal{T}_h^n \rightarrow \mathbb{R}^5$:

$$U_h(t, \bar{x}) = \bar{U}_h(K_j(t_{n+1}^-)) + \tilde{U}_h(\bar{x}, t), \qquad \forall (\bar{x}, t) \in \mathcal{K}_j^n,$$

such that:

$$\bar{U}_h(K_j(t_{n+1}^-)) = \hat{U}_0,$$

$$\int_{K_j(t_{n+1}^-)} \tilde{U}_h(\bar{x}, t)\, dK = 0,$$

with $K_j(t_{n+1}^-)$ the space-time element at time t_{n+1}, where the minus sign indicates that the mesh can change discontinuously across space-time slabs.

Weak Formulation

The weak formulation for the space-time discontinuous Galerkin finite element discretization can be formulated as:

- Find a $U_h \in V_h^1(\mathcal{T}_h^n)$, such that for all $W_h \in V_h^1(\mathcal{T}_h^n)$, the following variational equation is satisfied:

$$\sum_{n=0}^{N_T} \sum_{j=1}^{N_n} \{ \int_{\mathcal{K}_j^n} W_h^T \cdot \operatorname{div} \mathcal{F}(U_h)\, d\mathcal{K} + \int_{\mathcal{K}_j^n} (\operatorname{grad} W_h)^T \cdot \mathfrak{D}(U_h) : \operatorname{grad} U_h \, d\mathcal{K} \} = 0.$$

  The dyadic product is defined as $A : B = A_{ij} B_{ij}$ for $A, B \in R^{n \times m}$.

- The second contribution is the stabilization operator.

Transformation of Weak Formulation into ALE Form

- If we introduce the relation:

$$W_h^T \cdot \operatorname{div} \mathcal{F}(U_h) = \operatorname{div} \left(W_h^T \cdot \mathcal{F}(U_h)\right) - \left(\operatorname{grad} W_h\right)^T : \mathcal{F}(U_h),$$

into the weak formulation and apply Gauss' theorem to the contribution resulting from the first term on the righthand side then we obtain:

$$\int_{\mathcal{K}_j^n} \operatorname{div} \left(W_h^T \cdot \mathcal{F}(U_h)\right) \, d\mathcal{K} = \int_{\partial\mathcal{K}_j^n} n_{\mathcal{K}} \cdot \left(\left(W_h^-\right)^T \cdot \mathcal{F}(U_h^-)\right) \, d(\partial\mathcal{K}),$$

where $n_{\mathcal{K}}$ is the unit outward normal vector at the boundary $\partial\mathcal{K}^n$.

Transformation of Weak Formulation into ALE Form

- The ALE formulation can now be obtained by calculating the normal vector $n_{\mathcal{K}}$.

  Given the parameterization $(\bar{x}, t) = G_K^n(\xi)$ for the space-time element.

  - The normal vector $n_{\mathcal{K}}$ at the element boundary $\mathcal{Q}$ is equal to:

$$n_{\mathcal{K}} = (\bar{n}_{\mathcal{K}}, -v \cdot \bar{n}_{\mathcal{K}}).$$

    with $\bar{n}_{\mathcal{K}}$ the space components of the space-time normal vector $n_{\mathcal{K}}$ and v the velocity of a point at the element boundary $\mathcal{Q}$.

  - At the surfaces $K_j(t_n^+)$ and $K_j(t_{n+1}^-)$ the normal vector is equal to:

$$n_{\mathcal{K}} = (0, 0, 0, \mp 1)^T.$$

ALE Weak Formulation

The ALE form of the weak formulation for the Euler equations of gas dynamics is equal to:

- Find a $U_h \in V_h^1(\mathcal{T}_h^n)$, such that for all $W_h \in V_h^1(\mathcal{T}_h^n)$, the following variational equation is satisfied:

$$\sum_{n=0}^{N_T}\sum_{j=1}^{N_n}\Big\{-\int_{\mathcal{K}_j^n}(\operatorname{grad} W_h)^T : \mathcal{F}(U_h)d\mathcal{K} + \int_{K_j(t_n^+)\cup K_j(t_{n+1}^-)} W_h^- \cdot \mathcal{F}^- n_{\mathcal{K}} dK$$

$$+\int_{\mathcal{Q}_j^n} W_h^- \cdot \left(\bar{\mathcal{F}}(U_h^-)\bar{n}_{\mathcal{K}} - \bar{n}_{\mathcal{K}}\cdot v U_h^-\right) d\mathcal{Q}$$

$$+\int_{\mathcal{K}_j^n}(\operatorname{grad} W_h)^T \cdot \mathfrak{D}(U_h) : \operatorname{grad} U_h \, d\mathcal{K}\Big\} = 0.$$

Introduction of Numerical Flux

- In the summation over the elements, the element faces occur twice and the flux at element faces is multi-valued.
- The multi-valued flux is replaced by a numerical flux:

$$
\begin{aligned}
H(U_h^-, U_h^+, v, n) &= H_{HLLC}(U_h^-, U_h^+, v, \bar{n}), && \text{if } \bar{n}_{\mathcal{K}} \neq 0, \\
&= \tfrac{1}{2} n_{\mathcal{K},4}(U_h^- + U_h^+) - \\
&\quad \tfrac{1}{2}|n_{\mathcal{K},4}|(U_h^+ - U_h^-), && \text{if } \bar{n}_{\mathcal{K}} = 0,
\end{aligned}
$$

with H_{HLLC} the HLLC-flux.

Wave Pattern in HLLC-Flux

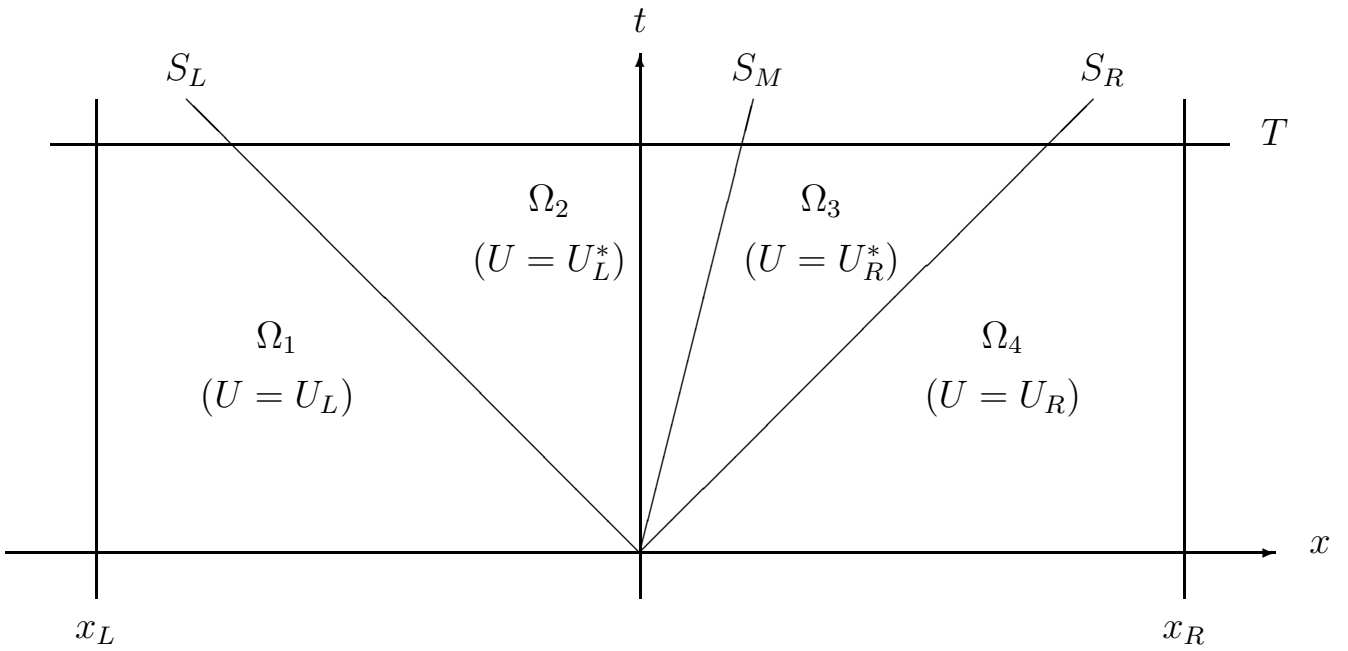

Wave pattern used in the definition of the HLLC flux function. S_L and S_R are the fastest left and right moving signal velocities. The solution in the star region U^* is divided by a wave with velocity S_M.

HLLC Flux

- The HLLC flux, introduced by Toro et al., is used as a numerical flux because it provides an accurate and efficient approximation to the Riemann problem.
- The HLLC flux at a moving interface is defined as:

$$H_{HLLC}(U_h^-, U_R^+, v, n) = \tfrac{1}{2}\Big(\hat{F}(U_L) + \hat{F}(U_R) - (|S_L - v| - |S_M - v|)U_L^* + (|S_R - v| - |S_M - v|)U_R^* + |S_L - v|U_L - |S_R - v|U_R - v(U_L + U_R))\Big).$$

  with $\hat{F} = \bar{n}_{\mathcal{K}}^T \bar{\mathcal{F}}$. In order to completely define the HLLC flux we still need to define the star states U_L^* and U_R^*, and the wave speeds S_L, S_R and S_M.
- See for instance P. Batten et al., On the choice of wave speeds for the HLLC Riemann solver *SIAM J. Sci. and Stat. Comp.* **18**, 1553-1570 (1997).

Weak Formulation

The weak formulation for the Euler equations of gas dynamics is now equal to:

Find a $U_h \in V_h^1(\mathcal{T}_h^n)$, such that for all $W_h \in V_h^1(\mathcal{T}_h^n)$, the following variational equation is satisfied:

$$\sum_{j=1}^{N_n} \Big\{ - \int_{\mathcal{K}_j^n} (\text{grad}\, W_h)^T : F(U_h) d\mathcal{K} + \int_{K_j(t_{n+1}^-)} W_h^- \cdot U_h^- dK$$

$$- \int_{K_j(t_n^+)} W_h^- \cdot U_h^+ dK + \int_{\mathcal{Q}_j^n} W_h^- \cdot H_{HLLC}(U_h^-, U_h^+, v, \bar{n}_{\mathcal{K}}) d\mathcal{Q}$$

$$+ \int_{\mathcal{K}_j^n} \big((\text{grad}\ W_h)^T \cdot \mathfrak{D}(U_h) \big) : \text{grad}\, U_h \, d\mathcal{K} \Big\} = 0.$$

Equations for the Flow Field Expansion Coefficients

- If we introduce the polynomial expansions for U_h and W_h into the weak formulation of the Euler equations and use the splitting into an element mean and a fluctuating part then the following set of equations for the coefficients of the element mean $\bar{U}_i(K_j(t^-_{n+1}))$ are obtained:

$$\left|K_j(t^-_{n+1})\right| \bar{U}_i(K_j(t^-_{n+1})) - \int_{K_j(t^+_n)} U_h(t^-_n, \bar{x}) dK + \int_{\mathcal{Q}^n_j} H_i(U^-_h, U^+_h, v, \bar{n}_{\mathcal{K}}) d\mathcal{Q} = 0.$$

- If the grid motion is continuous in time then these equations have the same structure as a first order accurate finite volume discretization.

Solution of Non-Linear DG Expansion Coefficient Equations

- The equations for all expansion coefficients can be expressed as:

$$\mathcal{L}(\hat{U}(\mathcal{K}^n), \hat{U}(\mathcal{K}^{n-1})) = 0.$$

- The non-linear equations of the space-time discretization are solved by augmenting them with a pseudo-time derivative:

$$\frac{\partial \hat{U}(\mathcal{K}_j^n)}{\partial \tau} = -\frac{1}{\triangle t}\mathcal{L}(\hat{U}(\mathcal{K}^n), \hat{U}(\mathcal{K}^{n-1}))$$

  The system is integrated in pseudo-time to a steady state using an optimized Runge-Kutta scheme in combination with a FAS multigrid algorithm to accelerate convergence.

- On the coarse meshes only the equations for element mean are used. Depending on the type of artificial dissipation we must, however, modify the Runge-Kutta scheme.

Stabilization Operator

- The effectiveness of the stabilization operator $\mathcal{D}$ strongly depends on the artificial viscosity matrix $\mathfrak{D} \in \mathbb{R}^{4\times4}$. The definition of the artificial viscosity matrix is more straightforward if the stabilization operator acts independently in all computational coordinate directions. This is achieved by introducing the artificial viscosity matrix $\tilde{\mathfrak{D}} \in \mathbb{R}^{4\times4}$ in computational space using the relation:

$$\mathfrak{D}(U_h|_{\mathcal{K}_j^n}, U_h^*|_{\mathcal{K}_j^n}) = R^T\, \tilde{\mathfrak{D}}(U_h|_{\mathcal{K}_j^n}, U_h^*|_{\mathcal{K}_j^n})\, R,$$

  where the matrix $R \in \mathbb{R}^{4\times4}$ is defined as:

$$R = 2\, H^{-1}\, \mathrm{grad}\, G_K.$$

- The matrix $H \in \mathbb{R}^{4\times4}$ is used introduced to ensure that both $\mathfrak{D}$ and $\tilde{\mathfrak{D}}$ have the same mesh dependence, and is defined as:

$$H = \mathrm{diag}\,(h_0, h_1, h_2, h_3).$$

Artificial Viscosity Model I

- In the artificial viscosity model I only the jump in the pressure across the element faces is used. This technique works very well in subsonic and transsonic flows with weak shocks. The artificial viscosity matrix is defined as:

$$\tilde{\mathfrak{D}}_{qq}(U_h|_{\mathcal{K}_j^n}, U_h^*|_{\mathcal{K}_j^n}) = \frac{C'\,\lambda\,h_q}{|\mathcal{Q}_j^n|}\sum_{m=1}^{6}\frac{|\,p^+(x_{(m)}) - p^-(x_{(m)})|\,|\mathcal{S}_m|}{p^+(x_{(m)}) + p^-(x_{(m)})}, \quad q = 1,2,3,$$

$$= 0, \qquad \text{otherwise.}$$

- The scaling factor λ is defined as: $\lambda = |\bar{n}_{\mathcal{K}} \cdot (u - v)| + c$, and is the maximum of the eigenvalues of the flux Jacobians $\partial\hat{\mathcal{F}}/\partial U$ at the midpoints at the midpoints $x_{(m)}$ of the faces $\mathcal{S}_m$.

Artificial Viscosity Model II

- For problems with stronger discontinuities the artificial viscosity model proposed and analyzed by Jaffre, Johnson and Szepessy, *Math. Models and Meth. in Appl. Sci*, **158**, pp. 81-116 (1998), is used. In this model both the jumps at the element faces and the element residual are used to define the artificial viscosity:

$$\tilde{\mathfrak{D}}_{qq}(U_h|_{\mathcal{K}_j^n}, U_h^*|_{\mathcal{K}_j^n}) = \max\big(C_2 h_{\mathcal{K}}^{2-\beta} R_q(U_h|_{\mathcal{K}_j^n}, U_h^*|_{\mathcal{K}_j^n})\,,\, C_1 h_{\mathcal{K}}^{\frac{3}{2}}\big), \quad q = 1,2,3,$$

$$= 0, \qquad \text{otherwise,}$$

with

$$R(U_h|_{\mathcal{K}_j^n}, U_h^*|_{\mathcal{K}_j^n}) = \Big|\sum_{k=0}^{3} \frac{\partial \mathcal{F}(U_h)}{\partial U_{h,i}} \frac{\partial U_{h,i}(G_K(0))}{\partial x_k}\Big| + \frac{C_0}{h_{\mathcal{K}}}\big|U_h^+(x_{(7)}) - U_h^-(x_{(7)})\big| +$$

$$\sum_{m=1}^{6} \frac{1}{h_{\mathcal{K}}}\big|\bar{n}_{\mathcal{K}}^T \mathcal{F}(U_h^+(x_{(m)})) - \bar{n}_{\mathcal{K}}^T \mathcal{F}(U_h^-(x_{(m)}))\big|.$$

Sod's Shock Tube Problem

Example: Sod's shock tube problem

- Initial conditions:

$$\rho_L = 1.0, \qquad \rho_R = 0.125$$
$$u_L = 0.0, \qquad u_R = 0.0$$
$$p_L = 1.0, \qquad p_R = 0.1$$

- Mesh size 100 elements in space.
- CFL number physical time step $CFL_{\triangle t} = 0.9$.
- The mesh is refined twice during the first time step, resulting in 21 extra elements.
- For the remaining time steps one refinement level is used.
- Dissipation model II is used.

Sod's Shock Tube Problem

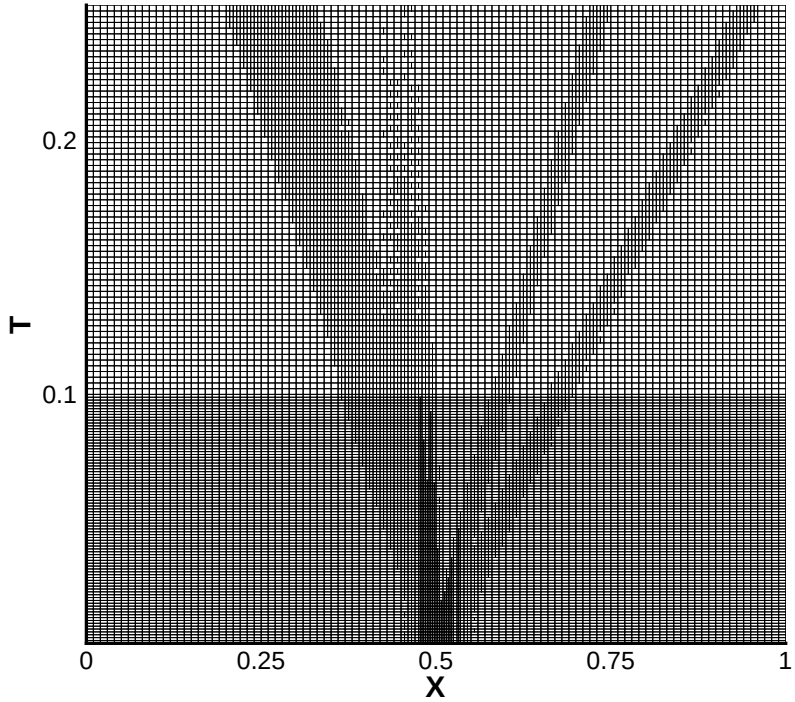

Space-time mesh for the adaptive solution of Sod's shock tube problem.

Sod's Shock Tube Problem

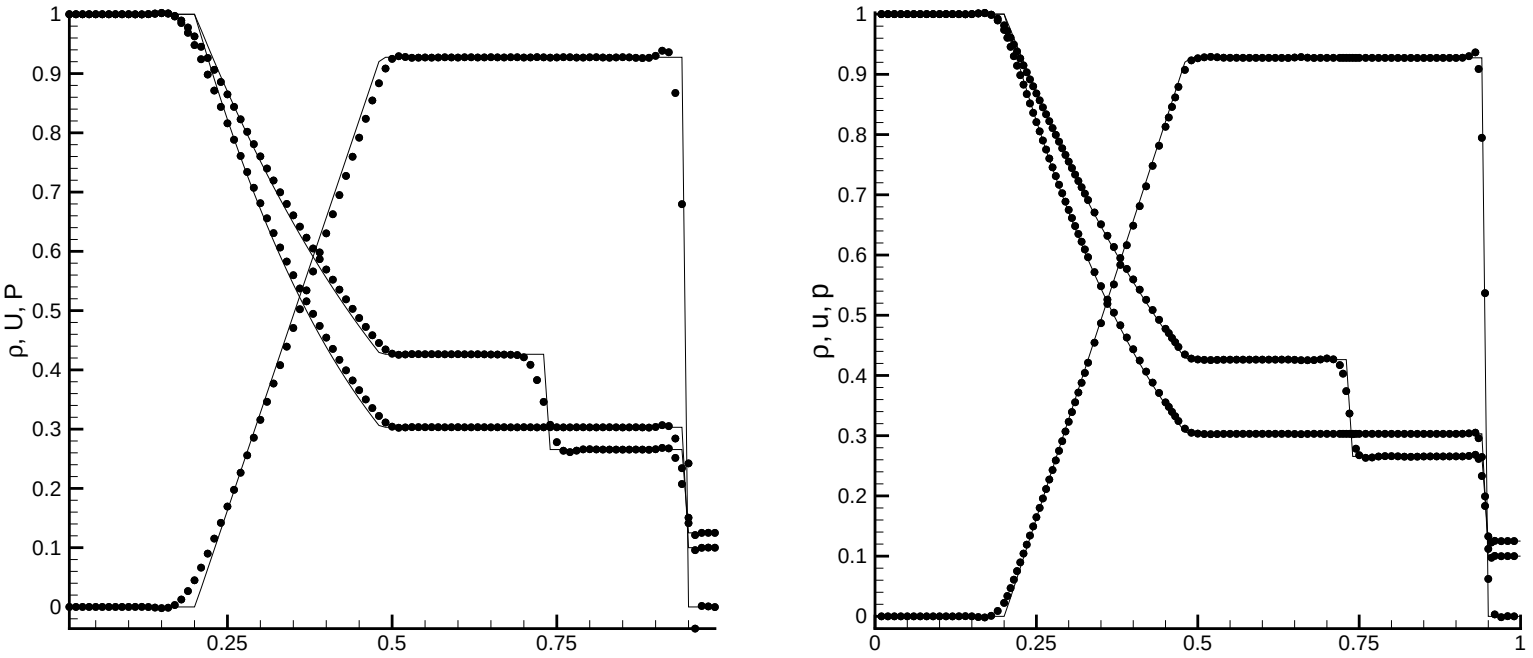

Sod's shock tube problem at $t = 0.2531$ on a uniform (left) and adapted mesh (right). Computed results plotted as circles, exact solution plotted as lines.

Conclusions

The space-time discontinuous Galerkin methods has the following interesting properties:

- Conservative numerical discretization on moving and deforming meshes which satisfies the geometric conservation law.
- Provides a local, element based discretization which is suitable for h-(p) mesh adaptation.
- Pseudo-time integration, in combination with multigrid acceleration (Lecture 2), is an efficient technique to solve the non-linear equations for the DG expansion coefficients and preserves the locality of DG methods.

Conclusions

- A semi-implicit Runge-Kutta scheme is necessary to maintain stability for small values of $\triangle\tau/\triangle t$ and optimized RK coefficients significantly improve the performance of the pseudo-time integration technique.
- The use of a stabilization operator in stead of a slope limiter makes it possible to converge to machine accuracy for steady state problems, whereas a limiter prevents convergence to steady state and reduces accuracy in a large part of the domain (see examples in Lecture 3).

Conclusions

Discontinuous Galerkin methods have the following disadvantages:

- More independent variables are required per element than for finite volume methods (for a second order accurate discretization five times more for the STDG FEM). This is partly compensated by the higher accuracy of discontinuous Galerkin finite element methods, grid adaptation and a better computational efficiency (Lecture 3).
- The standard DG formulations require more flux evaluations than finite volume methods, but for second order accurate discretizations it is possible to reduce this to one flux evaluation per element (face), which is equivalent with finite volume methods (Lecture 2).
- The discretization technique is considerably more complicated than for finite volume methods.